Phase constitution and microstructure of Ce–Fe–B strip-casting alloy*

Yan Chang-Jiang(严长江)[a)b)], Guo Shuai(郭 帅)[a)b)], Chen Ren-Jie(陈仁杰)[a)b)], Lee Dong(李 东)[a)b)], and Yan A-Ru(闫阿儒)[a)b)†]

[a)] *Key Laboratory of Magnetic Materials and Devices, Ningbo Institute of Material Technology and Engineering, Chinese Academy of Sciences, Ningbo* 315201, *China*

[b)] *Zhejiang Province Key Laboratory of Magnetic Materials and Application Technology, Ningbo Institute of Material Technology and Engineering, Chinese Academy of Sciences, Ningbo* 315201, *China*

(Received 19 December 2013; revised manuscript received 28 March 2014; published online 10 August 2014)

The strip-casting technique plays an important role in fabricating high coercivity sintered magnet. In this paper, we investigate the phase constitution and the microstructure of rapidly solidified Ce–Fe–B alloy fabricated by strip-casting. We find that the $Ce_2Fe_{14}B$ phase coexists with Fe, Fe_2B, and $CeFe_2$ phases in the Ce–Fe–B strips. The eutectic structure consisting of Fe and Fe_2B is encased in $Ce_2Fe_{14}B$ grains, which is blocked by the $CeFe_2$ grains at triple junctions, indicating that the microstructure of Ce–Fe–B strip is characteristic of a peritectic solidification. Thermal analysis indicates that the large supercooling of $Ce_2Fe_{14}B$ results in the residual Fe and Fe_2B. The microstructural optimization in Ce–Fe–B strips without Fe and Fe_2B could be achieved by a heat treatment of 1000 °C.

Keywords: magnetic material, Ce–Fe–B, microstructure, rapid solidification

PACS: 75.50.Ww **DOI:** 10.1088/1674-1056/23/10/107501

1. Introduction

$Nd_2Fe_{14}B$-type magnets have received much technical and scientific attention in the past three decades due to its high energy product.[1–4] Up to now, these traditional magnets have closely relied on scarce elements such as Nd, Pr, Dy, and Tb.[5–11] However, a growing demand for Nd–Fe–B magnets in miniaturization and energy conversion applications causes unbalanced utilization of rare-earth sources.[12–14] In the past years, many investigations have indicated that it is feasible to solve this problem by replacing Nd/Pr with other more abundant elements, such as La or Ce.[15–17] It was reported that $Ce_2Fe_{14}B$ phase is more stable than $La_2Fe_{14}B$ phase.[18] Therefore, Ce–Fe–B is chosen and studied in this paper.

As is well known, the powder metallurgy process is a productive method to prepare sintered Nd–Fe–B magnets, compared with hot pressed and hydrogenation–disproportionation–desorption–recombination (HDDR) processes.[19] If Ce–Fe–B sintered magnets are prepared through the modified processing route of sintered Nd–Fe–B magnet successfully, then the challenges that balanced use of rare-earth source will become easy. The modern powder metallurgy route to the fabricating of high performance sintered Nd–Fe–B magnets includes strip-casting, hydrogen-decrepitating, jet-milling, aligning, sintering, and annealing.[20] The strip-casting technique plays an important role in refining the microstructure of the final magnets, by which the distribution of intergranular phases is optimized and the α-Fe dendrites are suppressed in the rapidly solidification process.[21–23]

However, the phase diagram of Ce–Fe–B is different from that of Nd–Fe–B in several respects, and the vertical section of Ce–Fe–B system is not available,[19,24] indicating that the microstructure of Ce–Fe–B strip-casting alloy is different from that of Nd–Fe–B counterpart. It is primary to investigate the microstructure and phase constitution of starting alloy for preparing the sintered Ce–Fe–B magnets. In the present study, we prepare the Ce–Fe–B alloy by strip-casting, and investigate the microstructure and phase constitution of Ce–Fe–B strip-casting alloy. The microstructural difference between Ce–Fe–B and Nd–Fe–B alloys is also discussed. Meanwhile, we report an effort to optimize the microstructure of as-cast strips by heat treatment.

2. Experiments

According to 30 wt%–32 wt% Nd in Nd–Fe–B magnet,[5–8] in this study the nominal composition of the investigated alloy was $Ce_{30.5}Fe_{68.5}B_1$ (wt%) or $Ce_{14.16}Fe_{79.82}B_{6.02}$ (at.%). The alloy was prepared by strip-casting using a copper wheel with a speed of 1.8 m/s in an argon atmosphere. The induction melting temperature of the strip-casting measured by infrared thermometer was about 1280 °C, which is ∼ 200 °C higher than the melting point of $Ce_2Fe_{14}B$.[19] The average thickness of the resulting strips was about 200 μm. The microstructure of the strips was investigated by back scattered electron scanning electron microscope (BSE, SEM), as well as by high-resolution transmission electron microscopy (HRTEM). The chemical composition was

*Project supported by the National High Technology Research and Development Program of China (Grant No. 2011AA03A401).

†Corresponding author. E-mail: aruyan@nimte.ac.cn

© 2014 Chinese Physical Society and IOP Publishing Ltd

analyzed by an energy dispersive spectrometer (EDS). Crystallurgraphic structure and texture were identified by X-ray diffraction (XRD) with Cu-Kα radiation. Phase transformation behaviors in heating process and cooling process were measured by differential scanning calorimetry (DSC). The phase constitution and microstructure of strips after annealing at 1000 °C for 30 min were also analyzed.

3. Results and discussion

The XRD pattern from the plane near wheel side of $Ce_{30.5}Fe_{68.5}B_1$ strip is shown in Fig. 1. It can be seen that phases coexisting with the magnetic boride $Ce_2Fe_{14}B$ at room temperature are α-Fe, Fe_2B, $CeFe_2$, and Ce. The strongest peak of α-Fe indicates that fast cooling cannot suppress the precipitation of primary iron during rapid solidification. However, it should be noticed that strip-casting is an effective way to suppress this phase for Nd–Fe–B strip because the cooling rate of strip-casting technique is as high as 10^3 °C/s.[21] Besides, the $CeFe_2$ phase is also detected in the Ce–Fe–B melt-spun alloy and HDDR powder.[24,25] This suggests that controlling the cooling rate is not effective for the suppression of $CeFe_2$ phase. Meanwhile, a little residual Ce content is detected in the strip because the content of Ce in nominal composition is higher than that in the stoichiometric $Ce_2Fe_{14}B$ phase. Furthermore, the strength of (006) peak of $Ce_2Fe_{14}B$ phase is weaker than that of (410), suggesting that in Ce–Fe–B strip the fiber texture of $Ce_2Fe_{14}B$ along $\langle 00l \rangle$ direction is weak, which is different from the fiber texture along the $\langle 00l \rangle$ direction in $Nd_2Fe_{14}B$ strip.[22]

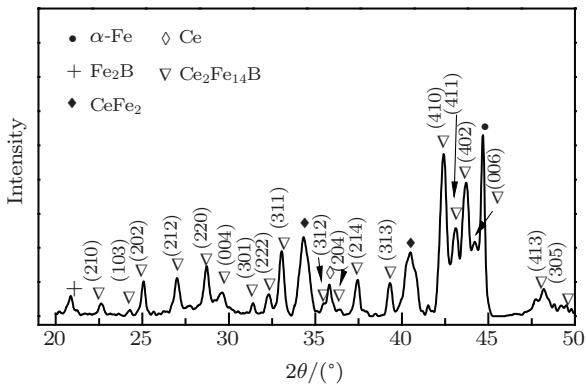


Fig. 1. XRD pattern from the plane near wheel side of as-casted $Ce_{30.5}Fe_{68.5}B_1$ strip.

Typical microstructures on cross section of as-cast $Ce_{30.5}Fe_{68.5}B_1$ strip are shown in Figs. 2(a) and 2(b). It can be seen that there are black, grey, and white contrasted regions in the BSE images. Besides, the grey dendrites surround the black dendrites and approach to white contrasted regions. The sizes of the black dendrites in the wheel side layer are smaller than those in the middle and free side layers of the strip [Fig. 2(a)]. Possibly the growth of black dendrites on wheel side is suppressed because of the faster cooling rate. The cooling rate of free side layer is faster than that of middle layer because of the lower heat conductivity of Ce, so the black dendrites in the middle layer are bigger than those in the free side layer.

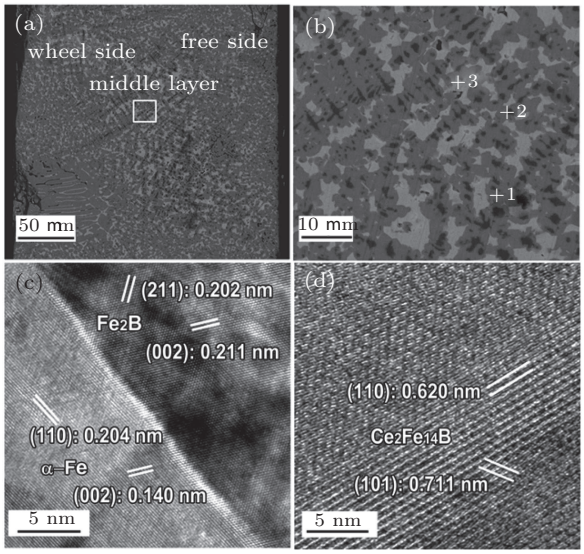


Fig. 2. Microstructures of $Ce_{30.5}Fe_{68.5}B_1$ as-cast strip. (a) BSE images on cross section of the strip. (b) The enlarged rectangular area in panel (a). HRTEM image of black dendrite (c) and grey dendrite (d) in image (a). The numbers marked in image (b) are the areas of EDS analysis.

To investigate the difference in regions according to the contrast, EDS analysis is performed on the three regions marked 1, 2, and 3 in Fig. 2(b) and the results are listed in Table 1. Because it is difficult to quantitatively determine the boron content by EDS, the black dendrites may contain Fe and Fe boride. The mixtures at triple junctions presenting a white contrast are a Ce and $CeFe_2$ compound. In addition, it can be concluded that the region with grey contrast corresponds to the $Ce_2Fe_{14}B$ phase, which does not form platelet-like structure penetrating from wheel side to free side. This is the reason why there is no fiber texture of $Ce_2Fe_{14}B$ in the strip.

Table 1. EDS analysis on different regions marked in Fig. 2(b).

Regions	Elements/at.%		Ratio of Ce:Fe
	Ce	Fe	
1	13.68	86.32	1:6.3
2	2.04	97.96	1:45.56
3	35.81	64.19	1:1.81

It can be seen that in Figs. 2(a) and 2(b) the black dendrite surrounded by $Ce_2Fe_{14}B$ phase is referred to as a "core-shell" structure. HRTEM analysis is performed to investigate the phases on the "core" and "shell", respectively. Obviously, a lattice fringe crosses the image in Fig. 2(c). According to the measurement of d-spacing, the "core" is composed of α-Fe and Fe_2B (or named Fe-rich phase), and the "shell" corresponds to the $Ce_2Fe_{14}B$ phase [Fig. 2(d)]. This core-shell

structure suggests that $Ce_2Fe_{14}B$ is formed by a peritectic transition from the Fe-rich phase to liquid phase. Besides, the grey contrast region is observed with low area fraction in Fig. 2(a), indicating the $Ce_2Fe_{14}B$ phase with low volume fraction in the as-cast strip.

Compared with microstructural analysis of Nd–Fe–B strip-casting alloy investigated by Bernardi *et al*.,[22] three differences in structure between Ce–Fe–B and Nd–Fe–B strips are summarized, as follows. Firstly, compared with the SEM image of Ce–Fe–B, the SEM images of Nd–Fe–B strips display only grey contrast (corresponding to 2:14:1 phase) and bright contrast (corresponding to Nd-rich phase). Secondly, a few columnar structures consisting of $Ce_2Fe_{14}B$ can be observed near the wheel side in Ce–Fe–B strips; however, in Nd–Fe–B strips, a cone structure consisting of $Nd_2Fe_{14}B$ columnar structures originates from the nucleation site and grows towards the free side. Thirdly, in the Ce–Fe–B strip, a structure where most grey dendrites enclose the black dendrites and are blocked by the white regions is characteristic of peritectic solidification, but an eutectic structure is generally believed to be of Nd–Fe–B strip-casting alloy.

To further study the relationship between phase and microstructure in the as-cast Ce–Fe–B strips, a thermal analysis is conducted by DSC, and the results are shown in Figs. 3(a) and 3(b). Figure 3(a) shows the phase transition during heating from room temperature to 1300 °C at a constant heating rate of 40 K/min. Two weak endothermic transitions occurring at 150 °C and 750 °C correspond to the Curie temperatures of $Ce_2Fe_{14}B$ and Fe phases, respectively. Subsequently, an endothermic reaction related to the peritectic transition of $CeFe_2$ takes place at 896 °C (A). An extra wide endothermic peak is observed at about 980 °C. According to the phase analysis in Fig. 1 and the microstructural observation of the strips in Fig. 2, this peak might be associated with L+Fe_2B+γ-Fe→$Ce_2Fe_{14}B$. As the temperature is increased further, a large endothermic reaction is observed at 1074 °C (B). This peak may correspond to melting points of both $Ce_2Fe_{14}B$ phase and Ce_2Fe_{17} phase, whose melting points are very close to each other.[24,26] Finally, an endothermic peak indicating an eutectic transformation is detected at 1208 °C (C).

Figure 3(b) shows the DSC curve during cooling from 1300 °C to 700 °C at a rate of 40 K/min. Phase transitions of A and C are also detected at 876 °C and 1173 °C. It can be seen that there are two adjacent peaks at 982 °C and 970 °C, which are related to transition B on the heating curve. Compared with the scenario of the heating curve, phase transitions B and D are subject to serious supercooling. The supercooling is 92 °C for phase transition B and 104 °C for phase transition D. The weak exothermic reaction at 750 °C is related to the Curie temperature of α-Fe (Ce) which is lower than pure Fe because a little Ce solid dissolves in iron.[26] This is also proven by the EDS results shown in Table 1.

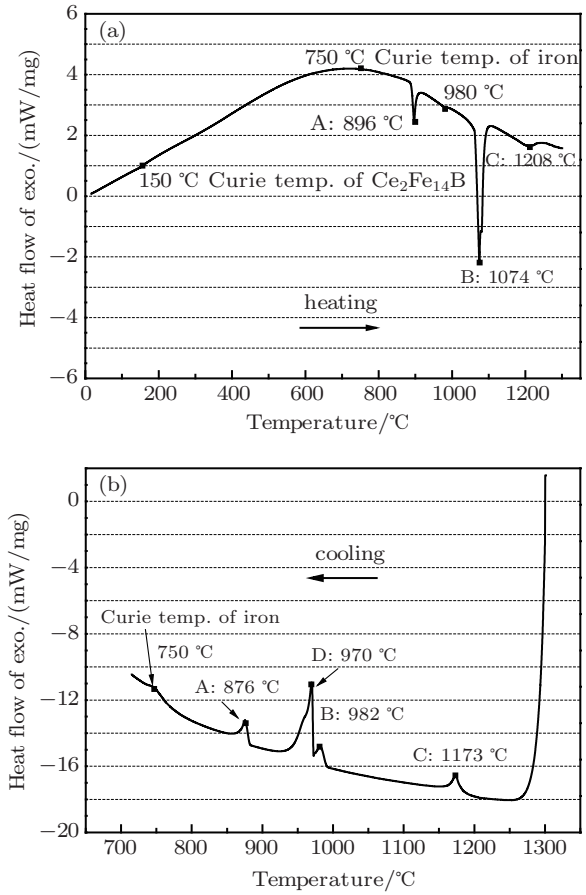


Fig. 3. DSC curves of the as-cast strip during heating from room temperature to 1300 °C at a rate of 40 K/min (a) and cooling from 1300 °C to 700 °C at 40 K/min (b). A, B, D denote the peritectic transitions and C represents the eutectic transition.

From the DSC analysis in the heating and cooling process, the mixture of Fe and Fe_2B is formed by the eutectic reaction L→ γ-Fe+Fe_2B at 1173 °C (C). The microstructure observations also show that the $Ce_2Fe_{14}B$ phase grains grow on the γ-Fe and Fe_2B dendrites. The peritectic transition to form $Ce_2Fe_{14}B$ is L+γ-Fe+Fe_2B→ $Ce_2Fe_{14}B$ (B). It should be noticed that this reaction does not happen until the temperature is below 982 °C. As a result, the Fe and Fe_2B dendrites cannot be effectively suppressed due to the big temperature gap referring to the eutectic transition (C) and the peritectic transition to form the $Ce_2Fe_{14}B$ (B), and this temperature gap is enlarged by supercooling the $Ce_2Fe_{14}B$.

The temperature that the strips deviated from the copper wheel is about 1000 °C. Then, the cooling rate of the strips decreased, resulting in an elongated time for the formation of $Ce_2Fe_{14}B$. Another peritectic transition $L'' + \gamma$-Fe →Ce_2Fe_{17}(D) between liquid and γ-Fe takes place at 970 °C, blocking the formation of $Ce_2Fe_{14}B$. It can be concluded that the temperature zone to form $Ce_2Fe_{14}B$ dendrites is as narrow

as 12 °C. Therefore, in the microstructure observation the area fraction of $Ce_2Fe_{14}B$ dendrites is low. Furthermore, Ce_2Fe_{17} is a metastable phase and easily transforms into $CeFe_2$ by $L'''+Ce_2Fe_{17} \rightarrow CeFe_2$(A). All of the transitions during cooling are listed in Table 2. It can be concluded that the peritectic microstructure of Ce–Fe–B strips is mainly due to the large temperature zone for the formation of Fe and Fe_2B. Suppressing the formation of these two phases can increase the volume fraction of $Ce_2Fe_{14}B$ phase, which can be achieved by quenching the strips in temperature gap I (between transitions C and B) and slowly cooling in temperature gap II (between transitions B and D). However, this two-step cooling is a challenge of the strip-casting technique.

Table 2. Summary of reactions detected in Fig. 3(b).

Phase	Type of reaction	Reaction formula	Temperature/°C
Fe_2B	Eutectic	$L \rightarrow \gamma$-Fe +Fe_2B	1173
Fe	Eutectic	$L \rightarrow \gamma$-Fe +Fe_2B	1173
$Ce_2Fe_{14}B$	Peritectic	$L' + \gamma$-Fe+$Fe_2B \rightarrow Ce_2Fe_{14}B$	982
Ce_2Fe_{17}	Peritectic	$L'' + \gamma$-Fe $\rightarrow Ce_2Fe_{17}$	970
$CeFe_2$	Peritectic	$L'''+Ce_2Fe17 \rightarrow CeFe_2$	876

Soft magnetic phase such as Fe and Fe_2B encased in 2:14:1 phase grains can subsequently weaken the alignment degree of final magnet.[21] Heat treatment is an effective way to eliminate the Fe in as-casted Nd–Fe–B starting alloy.[27] It is possible that heat treatment can also eliminate α-Fe and Fe_2B in as-cast Ce–Fe–B strips. Based on the thermal analysis, the annealing temperature should be higher than 980 °C but much lower than 1074 °C. So the heat treatment of strip is carried at 1000 °C for 30 min and then quenching in air. Figure 4(a) shows the XRD pattern of Ce–Fe–B strips after heat treatment. Compared with the pattern of as-cast strip in Fig. 1, characteristic peaks of α-Fe and Fe_2B disappear and the peaks of $Ce_2Fe_{14}B$ strengthen, which suggests α-Fe, Fe_2B and liquid phase constitutes the $Ce_2Fe_{14}B$ phase. There is also a little residual $CeFe_2$ content in the strip. The microstructure of Ce–Fe–B strip after heat treatment in Fig. 4(b) is consistent with that from the above phase analysis. It can be found that the grain size of $Ce_2Fe_{14}B$ phase is easier to enlarge after heat treatment.

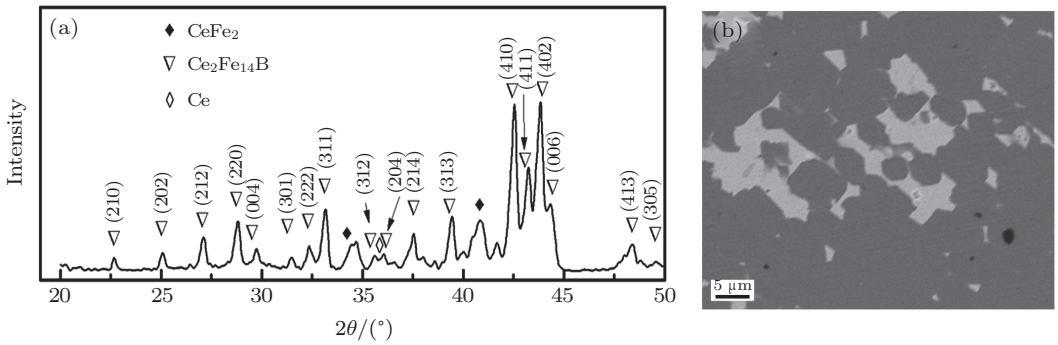


Fig. 4. XRD pattern (a) and BSE image (b) of Ce–Fe–B strip after annealing at 1000 °C for 30 min and quenching in air.

4. Conclusions

We systematically investigated the phase component and microstructure of $Ce_{30.5}Fe_{bal.}B_1$ strips. We have found that there are $Ce_2Fe_{14}B$, $CeFe_2$, α-Fe, Fe_2B, and Ce in as-cast strips. The microstructure of Ce–Fe–B strip-casting alloy is characteristic of a peritectic solidification because the $Ce_2Fe_{14}B$ phase grains surround a eutectic structure consisting of α-Fe and Fe_2B (or named Fe-rich phase) and are blocked by $CeFe_2$ phase grains at triple junction. Based on the thermal analyses and microstructure, heat treatment at 1000 °C is an effective way to optimize the microstructure of as-cast Ce–Fe–B strips without α-Fe and Fe_2B and to promote the formation of $Ce_2Fe_{14}B$ phase. Our further attempts aim to promote the formation of $Ce_2Fe_{14}B$ phase and suppress the precipitation of α-Fe and Fe_2B in Ce–Fe–B strips by alloying addition.

References

[1] Sagawa M, Fujimura S, Togawa N, Yamamoto H and Matsuura Y 1984 *J. Appl. Phys.* **55** 2083
[2] Wang Z, Gong W, Wang Y Z, Feng M Y, Wu Z, Hong Y and Cao Y 1985 *Chin. Phys. Lett.* **2** 79
[3] Matsuura Y 2006 *J. Magn. Magn. Mater.* **303** 344
[4] He Y Z 2013 *Chin. Phys. B* **22** 074101
[5] Li Y, Zhu M G, Li W, Zhou D, Lu F, Chen L, Wang J Y, Yan Q and Du A 2013 *Chin. Phys. Lett.* **30** 097501
[6] Gutfleisch O, Willard M A, Brück E, Chen C H, Sankar S G and Liu J P 2011 *Adv. Mater.* **23** 821
[7] Jang S M, Seo H J, Park Y S, Park H I and Choi J Y 2012 *IEEE Trans. Magn.* **48** 2933
[8] Chen B, Liu X, Chen R, Guo S and Yan A 2012 *J. Alloys Compd.* **516** 73
[9] Bai G, Gao R, Sun Y, Han G and Wang B 2007 *J. Magn. Magn. Mater.* **308** 20
[10] Lin C, Guo S, Fu W, Chen R, Lee D and Yan A 2013 *IEEE Trans. Magn.* **49** 3233
[11] He Y Z, Wu H P and Zou Z Q 2014 *Chin. Phys. B* **23** 047501
[12] Hu Z H, Lian F Z, Zhu M G and Li W 2008 *J. Magn. Magn. Mater.* **320** 1735

[13] Yue M, Liu W, Zhang D, Jian Z, Cao A and Zhang J 2009 *Appl. Phys. Lett.* **94** 092501
[14] Tang X, Hong L M and Zu D L 2010 *Chin. Phys. B* **19** 078702
[15] Buschow K H J 1986 *J. Less-Comm. Met.* **118** 349
[16] Li D and Bogatin Y 1991 *J. Appl. Phys.* **69** 5515
[17] Fuerst C, Capehart T, Pinkerton F and Herbst J 1995 *J. Magn. Magn. Mater.* **139** 359
[18] Yamada M, Kato H, Hiroyoshi H, Yamamoto H and Nakagawa Y 1987 *J. Magn. Magn. Mater.* **70** 328
[19] Sugimoto S 2011 *J. Phys. D: Appl. Phys.* **44** 064001
[20] Kaneko Y, Kuniyoshi F and Ishigaki N 2006 *J. Alloys Compd.* **408** 1344
[21] Guo S, Chen R, Zheng B, Yan G, Lee D and Yan A 2011 *IEEE Trans. Magn.* **47** 3267
[22] Bernardi J, Fidler J, Sagawa M and Hirose Y 1998 *J. Appl. Phys.* **83** 6396
[23] Fang Y K, Zhu M G, Guo Y Q, Li W and Han B S 2004 *Chin. Phys. Lett.* **21** 1655
[24] Herbst J, Meyer M and Pinkerton F 2012 *J. Appl. Phys.* **111** 07A718
[25] Xing M, Han J, Lin Z, Wan F, Li C, Liu S, Wang C, Yang J and Yang Y 2013 *J. Magn. Magn. Mater.* **331** 140
[26] Chuang Y, Wu C and Shao Z 1987 *J. Less Comm. Met.* **136** 147
[27] Scott D, Ma B, Liang Y and Bounds C 1996 *J. Appl. Phys.* **79** 4830